

F. Grimm, M. Stöhr, B. Noll, M. Aigner, R. Ewert, Semi-Analytical Prediction of Jet Flame Acoustics from Computational Fluid Dynamics Data, AIAA Journal 55 (2017) 2481-2487.

The final publication is accessible at

<http://dx.doi.org/10.2514/1.J055586>

On the AIAA web page

<http://www.aiaa.org/content.cfm?pageid=2>

the interested reader can find other material published by AIAA

A Semi-Analytical Approach for the Prediction of Jet Flame Acoustics from CFD Data

Felix Grimm^a and Michael Stöhr^b and Berthold Noll^c and Manfred Aigner^d
Institute of Combustion Technology, German Aerospace Center (DLR), 70569 Stuttgart, Germany

Roland Ewert^e
*Institute of Aerodynamics and Flow Technology,
German Aerospace Center (DLR), 38108 Braunschweig, Germany*

I. Introduction

Engine noise makes up the predominant fraction of aircraft sound emission [1, 2]. In particular, combustion noise is becoming a noise source in aero-engines with increasing relevance due to recent efforts of noise reduction of other components like the fan, turbine or the exhaust jet [3]. Up to now, particularly the mechanism of direct combustion noise production is poorly understood. However, there are numerous experimental [4–8], theoretical [3, 9, 10] and numerical studies [11–19] providing insights based on mainly fundamental and simple test cases. Nonetheless, no present study goes beyond empirical findings.

One possibility to account for combustion noise modeling is the use of analogy concepts. Sound propagation is described with fundamental mathematical relations. Noise source dynamics are then depicted with direct, unsteady simulations or modeled with statistical approaches. A compact way of describing noise source dynamics are so called correlation functions, expressing source development in convective processes by the influence of turbulence. In the presented paper, a semi-analytical approach for noise source modeling of diffusion jet-flames is introduced. It is based on derivations and considerations of high Mach number cold jet noise theories from Tam & Auriault [20], Morris

^a Research Engineer, Computer Simulation Department, felix.grimm@dlr.de

^b Research Engineer, Combustion Diagnostics Department, michael.stoehr@dlr.de

^c Head of Computer Simulation Department, berthold.noll@dlr.de

^d Professor, Director of the Institute, manfred.aigner@dlr.de

^e Head of Technical Acoustics Department, roland.ewert@dlr.de, AIAA Senior Member

& Farassat [21] and Morris & Boluriaan [22], and therefore extends existing, semi-empirical theories to the low Mach number regime which is typical for combustion noise problems.

Furthermore, the physical correlation function of combustion noise source dynamics is not known at present. Here, different theoretical constructs from the literature are discussed and a correlation similar to the one proposed by Tam et al. [20] is explicitly tested. The presented approach therefore contributes to the understanding of noise production and radiation and provides a theoretical tool for the analysis of all kinds of combustion noise source correlations. Measured sound pressure spectra of the open standard TNF DLR-A and DLR-B flames are compared not only to semi-analytical results, but also to literature similarity spectra [20]. The paper is structured as follows: First, several correlation functions from different models that are closely related to the presented approach are discussed and the choice of correlation function for the presented model is justified. Subsequently, the general spectrum for jet flame combustion noise is derived and the employed literature similarity spectra are introduced. Then, the TNF jet flame cases are described as well as the numerical CFD setup, results of which are input for the semi-analytical approach. The developed method is compared to theoretical and experimental data. It is found that the presented theory is in good agreement with experiments over a large range of frequencies and results are similar to literature model spectra [20]. In that context, a new set of measurement data of open DLR-A and -B flames is introduced.

II. Combustion Noise from an Acoustic Analogy Method

The analogy concept as introduced by Lighthill in the 1950s [23] describes sound p' generated by a forcing mechanism q and its propagation via certain characteristics, expressed by a wave operator \mathcal{L} ,

$$\mathcal{L}p'(\mathbf{x}, t) = q(\mathbf{x}, t). \quad (1)$$

In other words [24], it provides the connection between the far field with vanishing source terms and near field forcing emerging from sound created aerodynamically or, for combustion noise modeling, created by the interaction of chemistry and turbulence. With pressure spectra being defined as the

Fourier transform of the auto-correlation of acoustic pressure, the relation

$$\hat{S}(\mathbf{x}_1, \omega) = \int \int \int_{-\infty}^{\infty} \hat{G}_a^*(\mathbf{x}, \mathbf{x}_1, \omega) \hat{G}_a(\mathbf{x} + \mathbf{r}, \mathbf{x}_1, \omega) \langle q(\mathbf{x}, t_1) q(\mathbf{x} + \mathbf{r}, t_1 + \tau) \rangle \exp(i\omega\tau) d\tau d^n \mathbf{x} d^n \mathbf{r} \quad (2)$$

holds. $\langle \dots \rangle$ means ensemble averaging. $\hat{G}_a(\mathbf{x}, \mathbf{x}_1, \omega)$ is the harmonic Green's function of an adjoint set of equations [20] associated to the wave operator \mathcal{L} , dependent on the source position \mathbf{x} , an observer point \mathbf{x}_1 and the angular frequency ω . \mathbf{r} denotes the separation distance between sources. From Eq. (2) it becomes obvious that the cross-covariance is the only unknown for the determination of acoustic pressure spectra at arbitrary observer positions. The Green's functions are deterministically linked to the prescribed wave operator in a way that they provide the basic equations' fundamental solution.

Combustion noise sources are monopole radiators [3]. A local sudden increase of temperature causes rapid density changes and a response of the fluid medium in the form of acoustic pressure waves. In the presented study, this phenomenon is investigated based on jet flames. They are viewed under atmospheric conditions. Analogies can be reasonably drawn from cold jet noise models, since temperature fluctuations especially close to the flame root instantly respond to turbulent dynamics. A particularly suited theory therefore is the semi-analytical approach from Tam & Auriault [20]. Their model concept of sound radiation in high-speed turbulent jets relies on turbulent structures exerting perturbing pressure on the surrounding medium, $p_{turb} = \frac{2}{3}\rho k$. Those perturbations induced by turbulence blobs are responded by the fluid with compression and pressure fluctuations, resulting in acoustic waves. The convective noise source term of the Tam & Auriault model for no separation time and distance reads

$$\left\langle \left(\frac{Dq_s(\mathbf{x}, t_1)}{Dt_1} \right)^2 \right\rangle = c \frac{\rho^2 k^2}{\tau_s^2}. \quad (3)$$

Their associated semi-empirical correlation model function for turbulence induced noise sources in high-speed jets is

$$\left\langle \frac{Dq_s(\mathbf{x}, t_1)}{Dt_1} \frac{Dq_s(\mathbf{x} + \mathbf{r}, t_2)}{Dt_2} \right\rangle = \hat{R} \exp \left\{ -\frac{|\mathbf{r}_x|}{\bar{u}\tau} - \frac{\ln 2}{l_s^2} [(r_x - \bar{u}\tau)^2 + r_y^2 + r_z^2] \right\}, \quad (4)$$

which gives reasonably good agreement with measured correlation functions [20]. \mathbf{r} and τ are the separation distance and time between two points on the jet axis. \bar{u} and l_s denote mean source

convection velocity and local integral length scale. A similarly shaped correlation function for cold jet noise sources was presented by Morris & Boluriaan [22]. The term in the Tam & Auriault model describing evolving turbulence is $\exp(|r_x|/(\bar{u}\tau))$.

Their understanding of sources and evolving dynamics serve as an analogy for the presented approach for combustion noise. Jet flame combustion regimes are assumed to be dominated by turbulence, fast reactions and an instant response of combustion dynamics to turbulence [25]. Therefore, dynamics in cold and reacting jets are assumed to be comparable. A very similar correlation function of sources compared to the Tam & Auriault model is assumed at first, reading

$$\left\langle \frac{Dq_T(\mathbf{x}, t_1)}{Dt_1} \frac{Dq_T(\mathbf{x} + \mathbf{r}, t_2)}{Dt_2} \right\rangle = \hat{R} \exp \left\{ -\frac{|\tau|}{\tau_T} - \frac{\ln 2}{l_T^2} [(r_x - \bar{u}\tau)^2 + r_y^2 + r_z^2] \right\}. \quad (5)$$

The index T denotes combustion related in contrary to index s for cold jet noise. The combustion noise source term however has similar shape compared to the Tam & Auriault source but accounts for the turbulent temperature fluctuations as sound generation mechanism,

$$\left\langle \left(\frac{DT'^{m2}(\mathbf{x}, t_1)}{Dt_1} \right)^2 \right\rangle = \hat{R} = \frac{\widetilde{T'^{m2}}}{\tau_T^2}. \quad (6)$$

This source term formulation was introduced by Mühlbauer et al. [25] and used with a hybrid, stochastic approach for direct combustion noise prediction. As an extension of the cold jet noise model, Tam, Pastouchenko and Viswanathan published investigations for hot jets, featuring a different correlation function based on a modified Bessel function [26]. Their ansatz incorporates a jet temperature dependence of radiated noise due to the growth of Kelvin-Helmholtz instabilities in the mixing layer. The corresponding proposed correlation function reads

$$\begin{aligned} \left\langle \frac{Dq_s(\mathbf{x}, t_1)}{Dt_1} \frac{Dq_s(\mathbf{x} + \mathbf{r}, t_2)}{Dt_2} \right\rangle &= \\ &= \frac{2\hat{R}}{\Gamma(\nu)} \left(\frac{|r_x|}{2\bar{u}\tau_s} \right)^\nu K_\nu \left(\frac{|r_x|}{\bar{u}\tau_s} \right) \exp \left\{ -\frac{|r_x|}{\bar{u}\tau} - \frac{\ln 2}{l_s^2} [(r_x - \bar{u}\tau)^2 + r_y^2 + r_z^2] \right\}. \end{aligned} \quad (7)$$

K_ν is the modified Bessel function of order ν and $\Gamma(\nu)$ denotes the Gamma function. ν is an additional correlation parameter and Eq. (7) contains Eq. (4) for a choice of $\nu = 0.5$. Ewert et al. [27] propose a hybrid correlation model in order to account for the extended model by Tam et al. [26]. Their mixed correlation function or respectively the fraction of decorrelation due to evolving turbulence is

$$C_{mix} = \xi^2 C_1 + (1 - \xi^2) C_2, \quad (8)$$

with

$$C_1 = \exp\left(-\frac{|\tau|}{\tau_2}\right) \quad \text{and} \quad C_2 = \frac{1}{1-\mu} \left[\exp\left(-\frac{|\tau|}{\tau_1}\right) - \mu \exp\left(-\frac{|\tau|}{\tau_2}\right) \right], \quad (9)$$

$\mu = \tau_2/\tau_1$ is the ratio of two independent timescales, while τ_1 is associated to the integral scales from CFD simulations and the secondary timescale τ_2 is associated to decay processes on a Taylor micro-scale level. Therefore, μ is a correlation parameter of the Ewert et al. [27] model. For reacting jets, a variant of Eq. (9) is chosen, where the mixing parameter ξ is omitted, reading

$$\begin{aligned} \left\langle \frac{Dq_T(\mathbf{x}, t_1)}{Dt_1} \frac{Dq_T(\mathbf{x} + \mathbf{r}, t_2)}{Dt_2} \right\rangle &= \frac{\hat{R}}{1-\mu} \left[\exp\left(-\frac{|\tau|}{\tau_1}\right) - \mu \exp\left(-\frac{|\tau|}{\tau_2}\right) \right] \cdot \\ &\cdot \exp\left\{ -\frac{\ln 2}{l_T^2} [(r_x - u\tau)^2 + r_y^2 + r_z^2] \right\}. \end{aligned} \quad (10)$$

Values for the ratio of timescales were identified in preceding numerical studies by Grimm et al. [28, 29].

III. The Noise Spectrum for Jet Flames

In this section, the theoretical spectrum for jetflame noise is derived [30] as a function of flow field and combustion statistics in an acoustic source region with the correlation function of combustion noise sources, Eq. (10). The characteristic exponential turbulence related decay of the model is described by $(1/(1-\mu))[\exp(-|\tau|/\tau_1) - \mu \exp(|\tau|/\tau_2)]$. Equation (10) describes source convection in main flow direction. The wave number spectrum associated with Eq. (10) is

$$\begin{aligned} \hat{H}(\mathbf{x}, \boldsymbol{\alpha}, \omega) &= \\ &= \frac{1}{(2\pi)^3} \int \int_{-\infty}^{\infty} \left\langle \frac{Dq_T(\mathbf{x}, t_1)}{Dt_1} \frac{Dq_T(\mathbf{x} + \mathbf{r}, t_2)}{Dt_2} \right\rangle \exp(-i(\omega\tau - \boldsymbol{\alpha}\mathbf{r})) d\tau d^3r \end{aligned} \quad (11)$$

and integration for τ and \mathbf{r} gives

$$\begin{aligned} \hat{H}(\mathbf{x}, \boldsymbol{\alpha}, \omega) &= \\ &= \frac{2}{(2\pi)^3} \left(\frac{\pi}{\ln 2} \right)^{3/2} \frac{\hat{R}\tau_1 l_T^3 (1+\mu) \exp\left(-\frac{l_T^2 |\boldsymbol{\alpha}|^2}{4 \ln(2)}\right)}{1 + \omega^2 \tau_1^2 (1+\mu^2) (1 - \alpha_1 \frac{u_\infty}{\omega})^2 + \omega^4 \tau_1^4 \mu^2 (1 - \alpha_1 \frac{u_\infty}{\omega})^4}. \end{aligned} \quad (12)$$

With Eq. (2) it can be stated that

$$\begin{aligned} \hat{S}(\mathbf{x}_1, \omega) &= \int \int \int_{-\infty}^{\infty} \hat{G}_a^*(\mathbf{x}, \mathbf{x}_1, \omega) \hat{G}_a(\mathbf{x} + \mathbf{r}, \mathbf{x}_1, \omega) \\ &\quad \left\langle \frac{Dq_T(\mathbf{x}, t_1)}{Dt_1} \frac{Dq_T(\mathbf{x} + \mathbf{r}, t_2)}{Dt_2} \right\rangle \exp(i\omega\tau) d\tau d^3x d^3r. \end{aligned} \quad (13)$$

According to a far-field approximation [20, 22], information from consecutive downstream points can be inter-related with a phase difference from an observer point of view. This is depicted in Fig. 1. As a consequence, the Green's function at position $\mathbf{x} + \mathbf{r}$ can be expressed through its value at

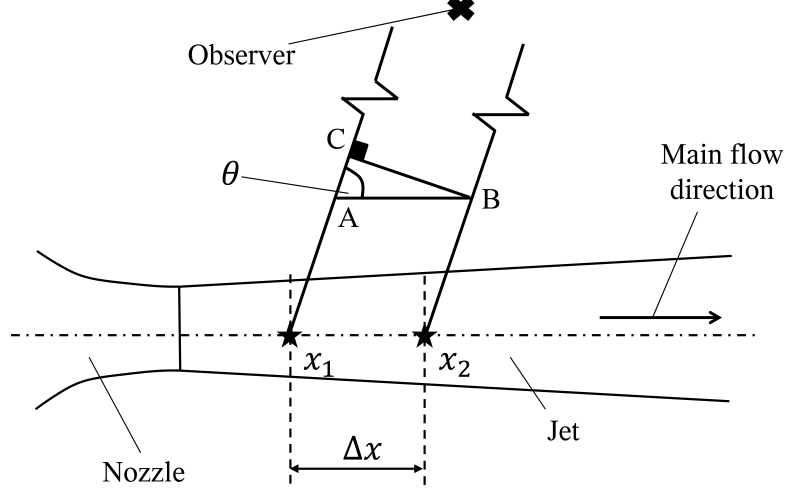


Fig. 1 Employed far-field condition for the analytical evaluation of jetflame pressure spectra [20, 22].

\mathbf{x} :

$$\hat{G}_a(\mathbf{x} + \mathbf{r}, \mathbf{x}_1, \omega) = \hat{G}_a(\mathbf{x}, \mathbf{x}_1, \omega) \exp\left(-i \frac{\omega \mathbf{x} \mathbf{r}}{c_0 |\mathbf{x}|}\right). \quad (14)$$

Subsequently, several steps of integration in Eq. (13) are performed, leaving the integral over the source coordinates \mathbf{x} only, consequently leading to an expression for far field spectra,

$$\hat{S}(\mathbf{x}_1, \omega) = 2 \left(\frac{\pi}{\ln 2}\right)^{3/2} \int_{V_s} \frac{(1 + \mu) \hat{R} \tau_1 l_T^3 |\hat{G}_a(\mathbf{x}, \mathbf{x}_1, \omega)|^2 \exp\left(-\frac{\omega^2 l_T^2}{4 \ln(2) c_0^2}\right)}{1 + \omega^2 \tau_1^2 (1 + \mu^2) (1 - M_c \cos \theta)^2 + \omega^4 \tau_1^4 \mu^2 (1 - M_c \cos \theta)^4} d^3 x. \quad (15)$$

The modulus of the Green's function in Eq. (15) is determined with the assumption of a quiescent background medium. It can be evaluated from a wave equation with right hand side forcing [30, 31], reading

$$\hat{G}_a(\mathbf{x}, \mathbf{x}_1, \omega) = -\frac{i\omega \exp(ik|\mathbf{x}_1 - \mathbf{x}|)}{c_0^2 4\pi |\mathbf{x}_1 - \mathbf{x}|}. \quad (16)$$

The modulus follows to

$$|\hat{G}_a(\mathbf{x}, \mathbf{x}_1, \omega)|^2 = \frac{\omega^2}{16\pi^2 c_0^4 |\mathbf{x}_1 - \mathbf{x}|^2}. \quad (17)$$

IV. Jet Flame Similarity Spectra

As summarized by Tam [9], shape of combustion noise spectra of open flames seem to be almost independent of configuration parameters like burner size, turbulence levels or type of fuels. Furthermore it was found that combustion noise spectra exhibit a similar spectral shape as cold high-speed jets [9, 10]. Due to that outcome, experimental pressure spectra are not only reproduced by the presented semi-analytical ansatz, but also compared to similarity spectra proposed by Tam, Golebiowski and Seiner [32], which were previously used for comparison with experimental combustion noise spectra [9]. Tam et al. found that jet mixing noise has two components. One is associated to large scale turbulent structures, while the other is linked to fine scale turbulence. Dependent on the angle of sound radiation relative to the jet axis, one of the two spectra is valid. A frequency resolved depiction of the similarity spectra is shown in Fig. 2. Tam et al. [32] found that for high

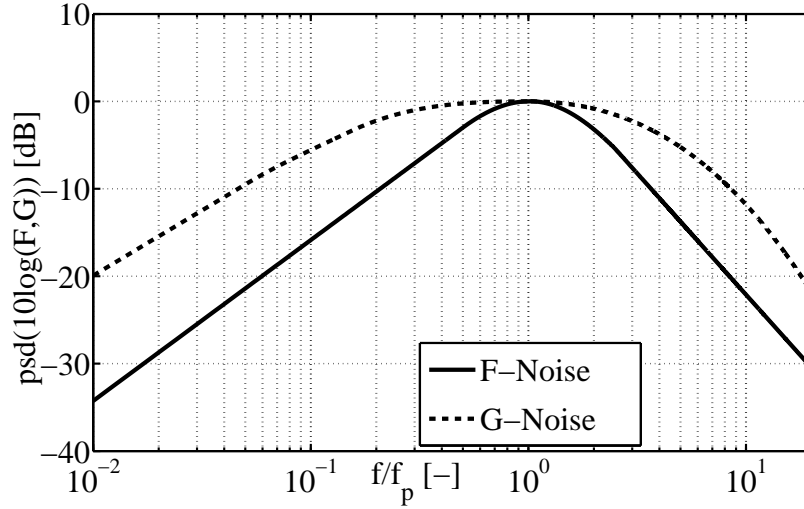


Fig. 2 Similarity spectra from Tam et al. [32].

speed cold jets, the G-spectrum, associated with fine scale turbulence, can be applied for smaller sound radiation angles, about normal to the jet axis. The F-spectrum from large scale turbulence gives a good representation of spectral shape for larger sound radiation directions, in the range of about $130 - 160^\circ$. For the comparison with experimental data from low Mach number reacting jets, Tam [9] applied the F-spectrum regardless of the sound radiation angle, finding good agreement over a wide range of frequencies for different observer positions.

V. Testcase Description and Numerical Model

Open, non-premixed, turbulent jet flames are investigated. The DLR-A flame is operated with a nitrogen diluted methane-hydrogen fuel mixture in air at atmospheric conditions ($T_\infty = 292K, p_\infty = 1\text{bar}$). The fuel composition is 22.1 Vol-% CH_4 , 33.2 Vol-% H_2 and 44.7 Vol-% N_2 . The stoichiometric mixture fraction is $Z_{st} = 0.167$ and the fuel is induced into the plenum through a pipe with diameter $D = 0.008m$, which is used as geometric reference. The burner is axis-symmetric and the fuel is induced with an average velocity $u_0 = 42.15m/s$, which yields a Reynolds number of about 15200. The setup for the DLR-B flame is identical except the mean fuel jet velocity is $u_0 = 63.2m/s$, yielding $Re = 22800$. The setup is shown in Fig. 3. For the acoustic pressure

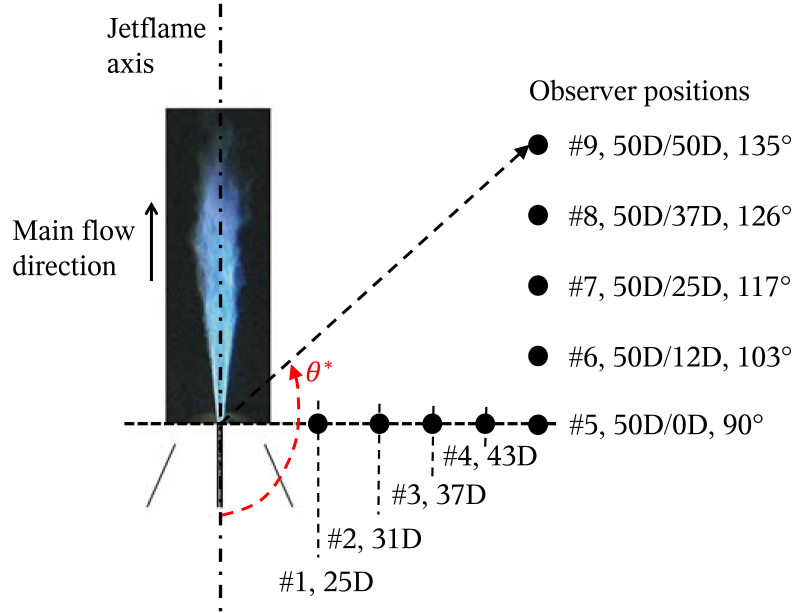


Fig. 3 Measured and modeled jet flame configuration with microphone positions and labeling conventions.

measurements, nine microphones (#1 – 9) are placed according to Fig. 3 where sound pressure spectra are evaluated with a sampling rate of $f = 200\text{kHz}$ over $t = 60\text{s}$. Brüel & Kjaer Type 4939 microphones are used.

VI. Specifications and Results of CFD Simulations

The CFD results as basis for the semi-analytical approach were conducted by Mühlbauer et al. [25]. Computational setup and simulation parameters can be found in the literature [25].

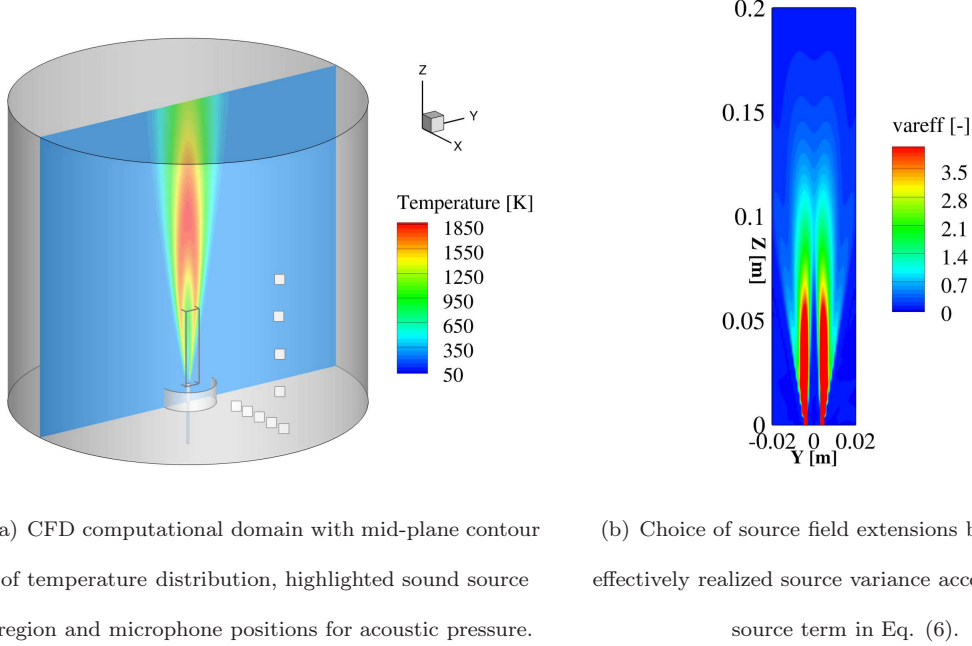
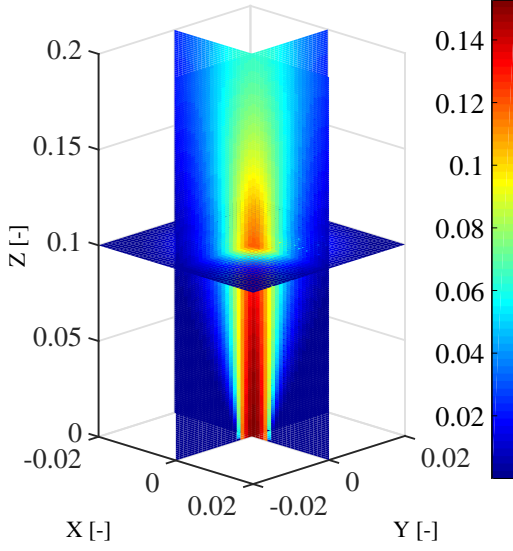
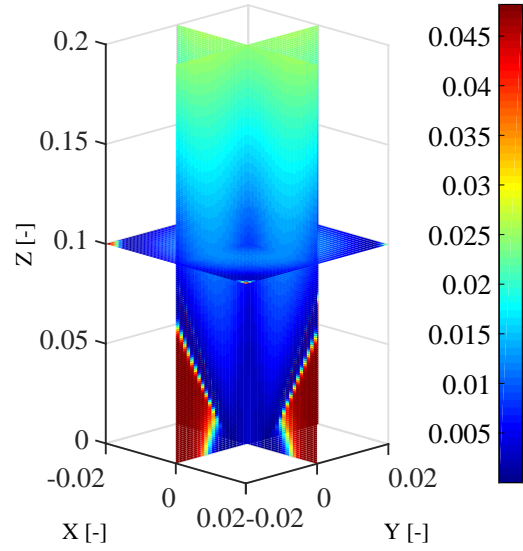


Fig. 4 CFD computational domain with sound source region, microphones (left) and choice of source field extensions (right) [25].

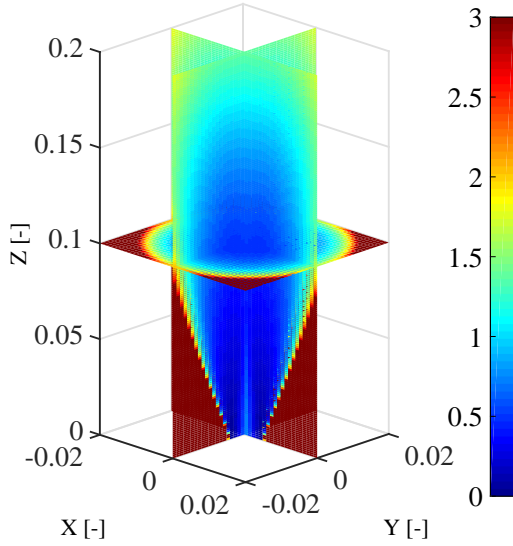
The CFD computational domain with highlighted sound source region and its choice of spatial extensions are shown in Fig. 4 together with the standard DLR-A and -B microphone positions. The distribution of jet velocities, combustion and turbulence statistics are displayed in Fig. 5 in order to show the distribution of flow field, combustion and turbulence statistics in the sound source region. The sound source region has the extensions $x, y \in [-0.02m; 0.02m]$ and $z \in [0m; 0.2m]$. It is therefore located directly downstream of the fuel pipe exit. As can be seen from the source convection field in Fig. 5a, sound sources close to the fuel pipe exit are convected primarily in jet axis direction, while the jet expands further downstream. Major contributions to sound pressure due to the effectively realized source variance are located close to the fuel jet axis (Fig. 4b). Therefore, the assumption of source convection in main flow direction only is justified for the analytical determination of sound pressure spectra. Turbulence statistics in Fig. 5b and 5c show a characteristic jet flame pattern, with increasing values with increasing distance to the fuel pipe exit. The temperature variance



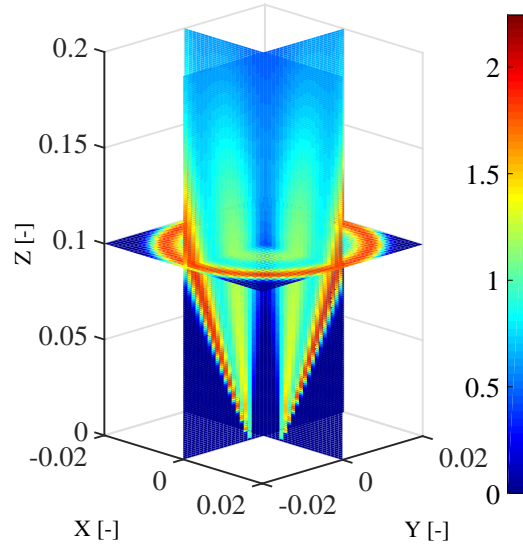
(a) Convection velocity u_z/c_{ref} .



(b) Integral length scales $(l_T f_{ref})/c_{ref}$.



(c) Integral timescales $\tau_T f_{ref}$.



(d) Distribution of temperature variance $\widetilde{T''^2}/T_{ref}^2$.

Fig. 5 Source field quantities extracted from CFD simulations, referenced to ambient quantities.

profile in Fig. 5d, which is used for local amplitude scaling of sound sources indicates the location of the reaction zone where large temperature gradients are present. A temperature variance field solution in the CFD RANS simulation is obtained by solving an additional transport equation, which reproduces experimental profiles with good agreement [25].

VII. The Semi-Analytical Model

Equation (15) provides a relation for frequency-resolved far field spectra as a function of source field quantities only, with the Green's functions as connection between sound source region and acoustic far field. It is

$$\hat{S}(\mathbf{x}_1, \omega) = f(\mathbf{x}_1, \mathbf{x}, \omega, \mathbf{u}_c, l_T, \tau_T, \mu, \theta^*). \quad (18)$$

The analogy for cold high-speed jets proposed by Tam & Auriault [20] requires further adaption in order to accurately reproduce their experimental data. Therefore they introduced calibration constants for the integral length- and timescales. In the presented study, the same specifications are used. Turbulence statistics and variance are evaluated with

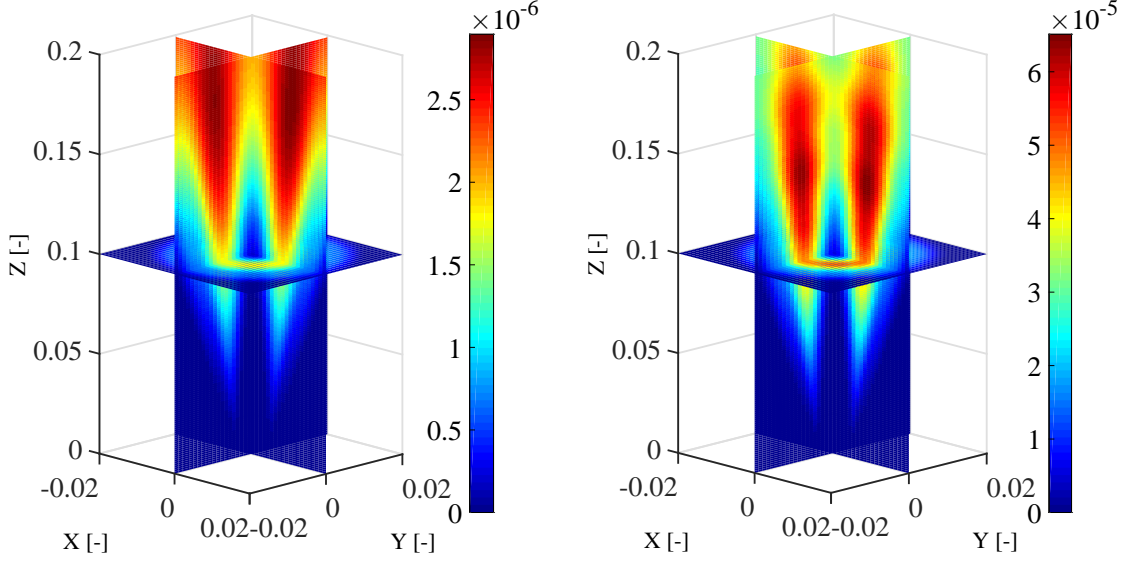
$$l_T = c_{Tl} \frac{k^{3/2}}{\epsilon} \quad \text{and} \quad \tau_T = c_{T\tau} \frac{k}{\epsilon} \quad \text{and} \quad \hat{R} = \frac{\widetilde{T'^2}}{\tau_T^2} \quad (19)$$

from the CFD simulation with the turbulent kinetic energy k and the turbulent dissipation ϵ . Here, $c_{T\tau} = 1$ and $c_{Tl} = c_{Tl, Tam}/M_c$, with $c_{Tl, Tam} = 0.256$. So to say, length scales are modified with the empirical constant of Tam & Auriault [20] divided by the average fuel nozzle Mach number $M_c = u_z/c_{ref}$, in order to conserve Strouhal-similarity of the predicted jet flame spectra [33]. Equation (15) is tested purely based on input from CFD RANS results as shown in section 5.

The angle of jet axis to observer position θ^* is determined from geometric relations and the parameter $\mu = \tau_2/\tau_1 = 1/7.93 = 0.1261$ [29] indicates the ratio of turbulent time scales. Spectra are evaluated by integrating the right hand side of Eq. (15) after inserting the field solutions of CFD simulations on the source region, as depicted in Fig. 5. The integrand of Eq. (15) is shown in Fig. 6 for exemplary frequencies. Figure 6 indicates that, as can be expected from the distribution of integral timescales representing turbulence dynamics in Fig. 5c, regions close to the flame root rather contribute to higher frequencies in the pressure spectra and vice versa.

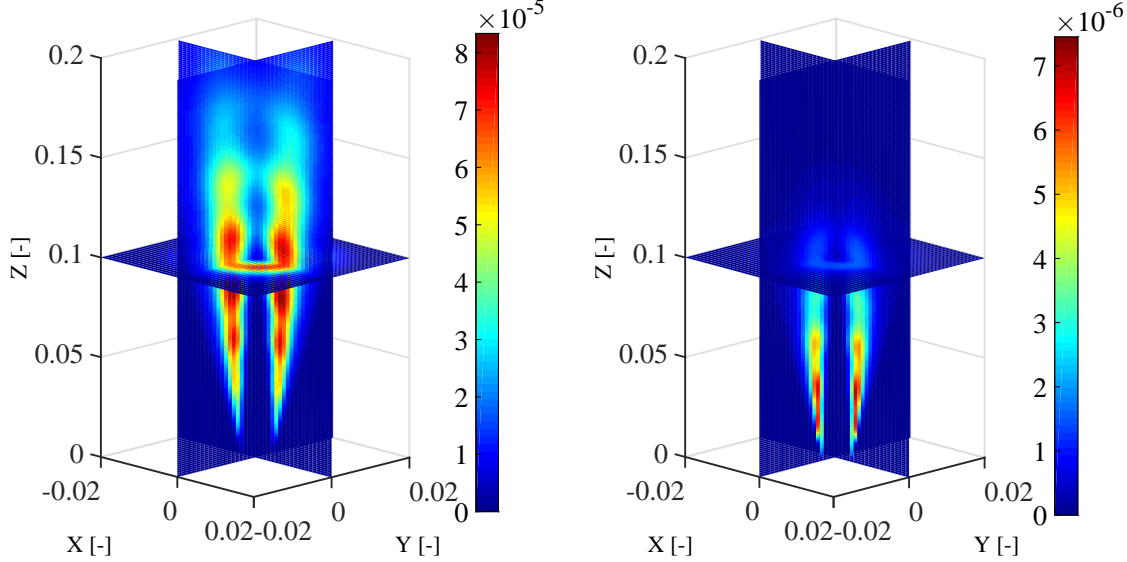
VIII. Comparison with Experiments

Semi-analytically evaluated pressure spectra are opposed to experimental data and similarity spectra from Tam et al. [32] in Figs. 7,8, and 9. Measurements do not provide anechoic boundaries, therefore uncertainties in the measured spectra especially for low frequencies are present. As stated



(a) Integrand of Eq. (15) for $f/f_{ref} = 10^{-2} = 3.5Hz$.

(b) Integrand of Eq. (15) for $f/f_{ref} = 10^{-1} = 35Hz$.



(c) Integrand of Eq. (15) for $f/f_{ref} = 10^0 = 345Hz$.

(d) Integrand of Eq. (15) for $f/f_{ref} = 10^1 = 3450Hz$.

Fig. 6 Integrand of Eq. (15) for the identification of frequency-resolved source contributions to the jet-flame noise spectra, referenced to $(c_{ref}^3 f_{ref}^2)/T_{ref}$.

by Tam [9], experimental pressure spectra in Figs. 7,8, and 9 are of similar shape despite different angles of attack, indicating that combustion noise is approximately isotropic. This observation also holds for the semi-analytically determined spectra. The shape of experimental pressure spectra in Figs. 7 to 9 are accurately captured by the G-spectrum over a large range of frequencies. Especially

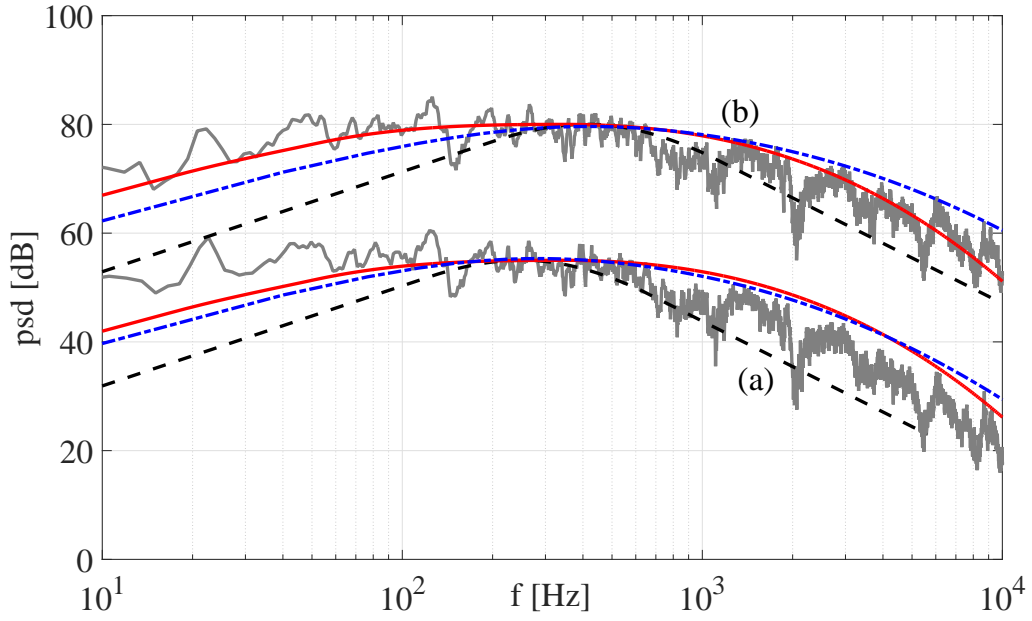


Fig. 7 Pressure spectra for DLR-A flame (a) and DLR-B flame + 20dB (b). Position #1, $25D/0D$, $\theta^* = 90^\circ$. Comparison of semi-analytical prediction (— · —), G-spectrum (—), F-spectrum (— —), and experiment (—).

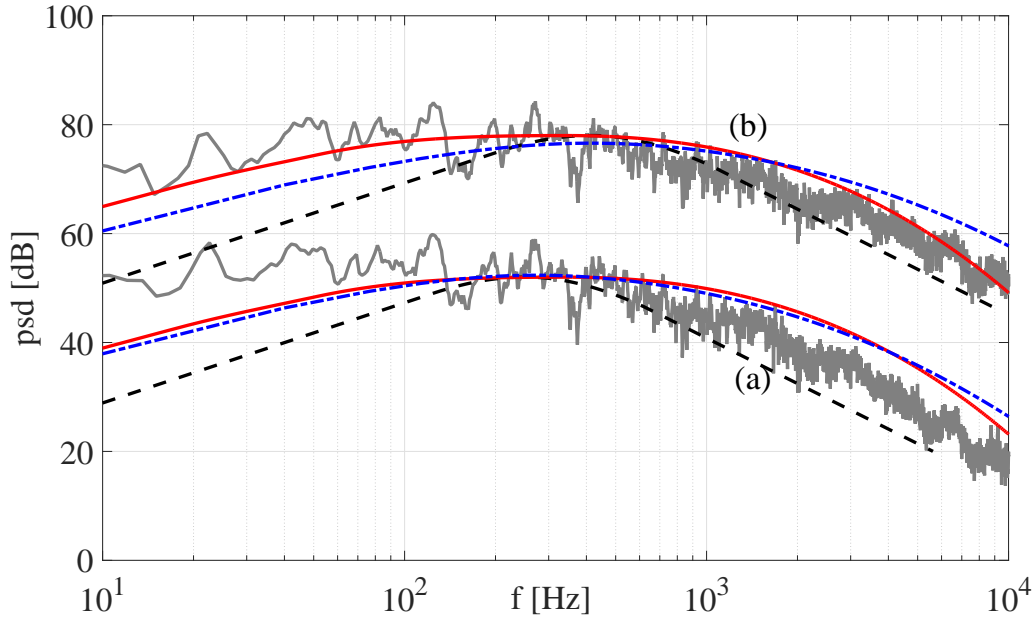


Fig. 8 Pressure spectra for DLR-A flame (a) and DLR-B flame + 20dB (b). Position #7, $50D/25D$, $\theta^* = 117^\circ$. Comparison of semi-analytical prediction (— · —), G-spectrum (—), F-spectrum (— —), and experiment (—).

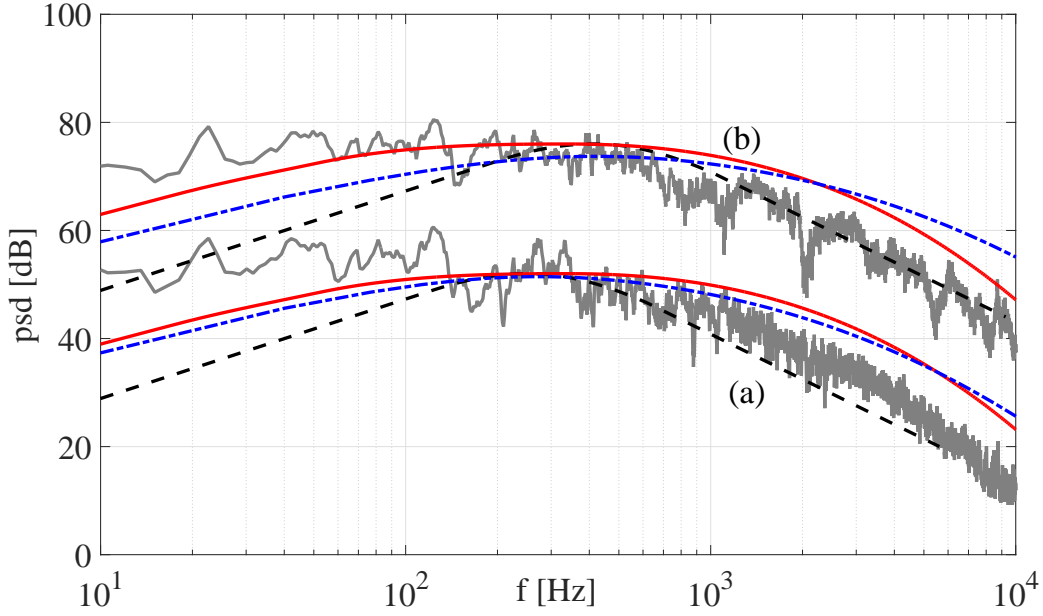


Fig. 9 Pressure spectra for DLR-A flame (a) and DLR-B flame + 20dB (b). Position #9, $50D/50D$, $\theta^* = 135^\circ$. Comparison of semi-analytical prediction (— · —), G-spectrum (—), F-spectrum (— —), and experiment (—).

for the downstream points in Figs. 8 and 9 with larger sound radiation angles, the F-spectrum matches with the slope of measured spectra for higher frequencies, however significantly disagrees for low frequencies.

The semi-analytical model reproduces the slope of experimental pressure spectra well, especially for mid- and high-frequency ranges for investigated observer positions with low angle of attack, as in Fig. 7. Deviations are present for larger sound radiation angles, as can be seen in Figs. 8 and 9. An explanation for this could be the assumption of a quiescent background flow with no density gradients. Therefore, refraction effects are not incorporated in the model at the present state.

The semi-analytical spectra are almost identical to the G-spectrum, as shown in Figs. 7 to 9, therefore matching the Tam et al. [20] theory. Uncertainties of the approach are due to assumptions like a quiescent background flow field and the accountancy for source convection in one predominant flow direction, but also due to deficiencies of the CFD RANS models. CFD turbulence input is required for the frequency resolved contribution to combustion noise, as was shown in Fig. 6. However, it is expected that the further downstream of the flame root, the less accurate the modeling of

integral turbulence statistics. This could imply uncertainties of the semi-analytical profiles for low frequencies.

The accountancy for Reynolds-scalability of the approach is shown by comparison with measurements of DLR-A and -B flame pressure spectra with a significantly different fuel pipe exit Reynolds number. In both cases (DLR-A and DLR-B), the slope of the measured pressure spectra is reproduced by the analytical approach with good quality. Either DLR-A and DLR-B spectra are analytically well described by the method without numerical calibration of the underlying correlation function.

IX. Conclusions

A semi-analytical method for the prediction of the spectral shape of jet flame acoustics was introduced. It relies on input of mean flow field and turbulence statistics from CFD simulations on an assumed sound source region and the knowledge of microphone positions relative to the sound source domain. The approach was inspired by well-established high-speed cold jet noise models and was shown to be a consistent low Mach number extension to those theories. Open TNF jet flame pressure spectra were reliably reproduced for a large range of frequencies and different sound radiation angles. Therefore, the presented approach was able to predict not only frequency-resolved combustion noise distribution but also noise radiation characteristics. Combustion noise source correlations are still not known, however were approximated with a model function relying on integral and intermediate timescales, closely related to correlation functions from the literature for hot jets. The good match between experimental and theoretical results indicate that the suggested correlation function is highly suited for combustion noise source modeling. The presented ansatz furthermore matched with well established, semi-empirical similarity spectra and is therefore in accordance with existing theoretical investigations on noise production and radiation. Due to the employment of CFD RANS simulation input of source field quantities, frequency resolved contributions of sound production and their impact to the shape of sound pressure spectra were identified. The new method therefore significantly contributes to the understanding of the process of turbulent combustion induced sound formation and radiation.

Acknowledgments

This collaborative work was supported within the project DECISIVE which is funded by the German Aerospace Center (DLR).

References

- [1] Rolls-Royce, *The Jet Engine*, Technical Publications Department, Rolls-Royce plc, Derby, England, 1996, ISBN 10: 0902121235.
- [2] Leylekian, L., Lebrun, M., and Lempereur, P., “An Overview of Aircraft Noise Reduction Technologies,” *Aerospace Lab Journal*, 2014, AL07-01, pp. 1-15, doi: 10.12762/2014.AL07-01.
- [3] Dowling, A. and Mahmoudi, Y., “Combustion noise,” *Proceedings of the Combustion Institute*, Vol. 35, 2015, pp. 65–100, ISSN 1540-7489, doi: 10.1016/j.proci.2014.08.016.
- [4] Kotake, S. and Takamoto, K., “Combustion Noise: Effects of the Shape and Size of Burner Nozzle,” *Journal of Sound and Vibration*, Vol. 112, No. 2, 1987, pp. 345–354, doi: 10.1016/S0022-460X(87)80201-8.
- [5] Kotake, S. and Takamoto, K., “Combustion Noise: Effects of the Velocity Turbulence of Unburned Mixture,” *Journal of Sound and Vibration*, Vol. 139, No. 1, 1990, pp. 9–20, doi: 10.1016/0022-460X(90)90771-Q.
- [6] Narayanan, S., Baber, T., and Polak, D., “High Subsonic Jet Experiments: Turbulence and Noise Generation Studies,” *AIAA Journal*, Vol. 40, No. 3, 2002, pp. 430–437, doi: 10.2514/2.1692.
- [7] Singh, K., Frankel, S., and Gore, J., “Effects of combustion on the sound pressure generated by circular jet flows,” *AIAA Journal*, Vol. 41, No. 2, 2003, pp. 319–321, doi: 10.2514/2.1949.
- [8] Singh, K., Frankel, S., and Gore, J., “Study of spectral noise emissions from standard turbulent non-premixed flames,” *AIAA Journal*, Vol. 42, No. 5, 2004, pp. 931–936, doi: 10.2514/1.3424.
- [9] Tam, C., “On the Spectrum of Combustion Noise,” *21st AIAA/CEAS Aeroacoustic Conference*, 2015, AIAA Paper 2015-2969, doi: 10.2514/6.2015-2969.
- [10] Mahan, J. and Karchmer, A., “Combustion and core noise,” *Aeroacoustics of Flight Vehicles: Theory and Practice*, Vol. 1, 1991, pp. 483–517.
- [11] Flemming, F., Sadiki, A., and Janicka, J., “Investigation of combustion noise using a LES/CAA hybrid approach,” *Proceedings of the Combustion Institute*, Vol. 31, 2007, pp. 3189–3196, doi: 10.1016/j.proci.2006.07.060.

- [12] Bui, T., Schröder, W., and Meinke, M., “Numerical analysis of the acoustic field of reacting flows via acoustic perturbation equations,” *Computers & Fluids*, Vol. 37, No. 9, 2008, pp. 1157–1169, doi: 10.1016/j.compfluid.2007.10.014.
- [13] Zhang, F., Habisreuther, P., Hettel, M., and Bockhorn, H., “Numerical Computation of Combustion Induced Noise Using Compressible LES and Hybrid CFD/CAA Methods,” *Acta Acustica united with Acustica*, Vol. 98, No. 1, 2012, pp. 120–134, doi: 10.3813/AAA.918498.
- [14] Brick, H., Piscoya, R., Ochmann, M., and Költzsch, P., “Prediction of the Sound Radiation from Open Flames by Coupling a Large Eddy Simulation and a Kirchhoff Method,” *Forum Acusticum*, 2005, pp. 85–89.
- [15] Liu, Y., Dowling, A., Swaminathan, N., and Dunstan, T., “Spatial correlation of heat release rate and sound emission from turbulent premixed flames,” *Combustion and Flame*, Vol. 159, 2012, pp. 2430–2440, doi: 10.1016/j.combustflame.2012.03.003.
- [16] Andersson, N., Eriksson, L.-E., and Davidson, L., “Large-Eddy Simulation of Subsonic Turbulent Jets and Their Radiated Sound,” *AIAA Journal*, Vol. 43, No. 9, 2005, pp. 1899–1912, doi: 10.2514/1.13278.
- [17] Lyrantzis, A., “Surface Integral Methods in Computational Aeroacoustics: From the (CFD) Near-Field to the (Acoustic) Far-Field,” *International Journal of Aeroacoustics*, Vol. 2, No. 2, 2003, pp. 95–128, doi: 10.1260/147547203322775498.
- [18] Hirsch, C., Wäsle, J., Winkler, A., and Sattelmayer, T., “A spectral model for the sound pressure from turbulent premixed combustion,” *Proceedings of the Combustion Institute*, Vol. 31, No. 1, 2007, pp. 1435–1441, doi: 10.1016/j.proci.2006.07.154.
- [19] Silva, C., Leyko, M., Nicoud, F., and Moreau, S., “Assessment of combustion noise in a premixed swirled combustor via Large-eddy simulation,” *Computers and Fluids*, Vol. 78, 2011, pp. 1–9, doi: 10.1016/j.compfluid.2010.09.034.
- [20] Tam, C. and Auriault, L., “Jet Mixing Noise from Fine-Scale Turbulence,” *AIAA Journal*, Vol. 37, No. 2, 1999, pp. 145–153, doi: 10.2514/2.691.
- [21] Morris, P. and Farassat, F., “Acoustic Analogy and Alternative Theories for Jet Noise Prediction,” *AIAA Journal*, Vol. 40, No. 4, 2002, pp. 671–680, doi: 10.2514/2.1699.
- [22] Morris, P. and Boluriaan, S., “The Prediction of Jet Noise from CFD Data,” *10th AIAA/CEAS Aeroacoustic Conference*, AIAA Paper 2004-2977, doi: 10.2514/6.2004-2977, May 2004.
- [23] Lighthill, M., “On sound generated aerodynamically. I. General Theory,” *Proceedings of the Royal Society*, Vol. A 211, 1952, pp. 564–587, doi: 10.1098/rspa.1952.0060.

- [24] Ewert, R., Dierke, J., Siebert, J., Neifeld, A., Appel, C., Siefert, M., and Kornow, O., “CAA broadband noise prediction for aeroacoustic design,” *Journal of Sound and Vibration*, Vol. 330, No. 17, 2011, pp. 4139–4160, doi: 10.1016/j.jsv.2011.04.014.
- [25] Mühlbauer, B., Ewert, R., Kornow, O., and Noll, B., “Evaluation of the RPM Approach for the Simulation of Broadband Combustion Noise,” *AIAA Journal*, Vol. 48, No. 7, 2010, pp. 1379–1390, doi: 10.2514/1.45535.
- [26] Tam, C., Pastouchenko, N., and Viswanathan, K., “Fine-Scale Turbulence Noise from Hot Jets,” *AIAA Journal*, Vol. 43, No. 8, 2005, pp. 1675–1683, doi: 10.2514/1.8065.
- [27] Ewert, R., Neifeld, A., and Wohlbrandt, A., “A three-parameter Langevin model for hot jet mixing noise prediction,” *18th AIAA/CEAS Aeroacoustics Conference*, AIAA Paper 2012-2238, doi: 10.2514/6.2012-2238, June 2012.
- [28] Grimm, F., Ewert, R., Dierke, J., Noll, B., and Aigner, M., “The Fast Random Particle Method for Combustion Noise Prediction,” *20th AIAA/CEAS Aeroacoustics Conference*, AIAA Paper 2014-2451, doi: 10.2514/6.2014-2451, June 2014.
- [29] Grimm, F., Ewert, R., Dierke, J., Noll, B., and Aigner, M., “Efficient Full 3D Turbulent Combustion Noise Simulation Based on Stochastic Sound Sources,” *21st AIAA/CEAS Aeroacoustics Conference*, AIAA Paper 2015-2973, doi: 10.2514/6.2015-2973, June 2015.
- [30] Ewert, R., “Private Communication,” German Aerospace Center DLR, Institute of Aerodynamics and Flow Technology, Technical Acoustics, 2013, 38108 Braunschweig.
- [31] Ewert, R., Neifeld, A., and Fritzsche, A., “A 3-D modal stochastic jet noise source model,” *17th AIAA/CEAS Aeroacoustics Conference*, AIAA Paper 2011-2887, doi: 10.2514/6.2011-2887, June 2011.
- [32] Tam, C., Golebiowski, M., and Seiner, J., “On the Two Components of Turbulent Mixing Noise from Supersonic Jets,” *2nd AIAA/CEAS Aeroacoustic Conference*, AIAA Paper 1996-1716, doi: 10.2514/6.1996-1716, May 1996.
- [33] Neifeld, A. and Ewert, R., “Jet mixing noise from single stream jets using stochastic source modeling,” *17th AIAA/CEAS Aeroacoustic Conference*, AIAA Paper 2011-2700, doi: 10.2514/6.2011-2700, June 2011.